

Electrochemical Study of Graphene Coated Nickel Foam as an Anode for Lithium-Ion Battery

A. Mukanova^{1,2}, A. Zharbossyn¹, A. Nurpeissova², S.-S. Kim³, M. Myronov⁴, Zh. Bakenov^{1,2,5*}

¹School of Engineering, Nazarbayev University, 53 Kabanbay Batyr Ave., Block 3, Astana 010000, Kazakhstan

²National Laboratory Astana, Nazarbayev University, 53 Kabanbay Batyr Ave., Block 6, Astana 010000, Kazakhstan

³Chungnam National University, 99 Daehak Ave., Daejeon, 34134, South Korea

⁴Physics Department, University of Warwick, Coventry CV4 7AL, United Kingdom

⁵Institute of Batteries, 53 Kabanbay Batyr Ave., Block 13, 010000, Astana, Kazakhstan

Article info

Received:

20 October 2017

Received in revised form:

24 December 2017

Accepted:

10 February 2018

Keywords:

graphene
nickel oxide
nickel foam
3D current collector
CVD
lithium-ion batteries

Abstract

This study reports the synthesis of a few-layered graphene (GF) thin film on Ni foam by chemical vapor deposition (CVD) technique and investigation of its electrochemical performance as a negative electrode for lithium-ion batteries (LIBs). A standard deposition procedure with a methane precursor was employed to prepare the GF films. The SEM studies revealed the formation of a dark uniform film on the surface of Ni foam's wires upon the CVD deposition. The film consisted of numerous GF sheets replicating the shape of the Ni grain boundaries over the Ni wire surface. The Raman spectroscopy of the prepared films on the Ni foam confirmed that the samples are a few-layered GF with high quality and purity. In order to evaluate the potential of the use of the prepared materials as an anode in LIBs, their electrochemical performance was studied in coin-type lithium half-cells using cyclic voltammetry (CV) and galvanostatic cycling. The results of CV showed that both graphene and native oxide layer (NiO) on nickel foam exhibit electrochemical activity with respect to lithium ions. Galvanostatic cycling revealed that both GF and NiO contribute to the overall capacity, which increases upon cycling with a stable Coulombic efficiency of around 99%. The designed 3D GF coated NiO/Ni anode demonstrated a gradual increase of its areal charge capacity from 65 $\mu\text{Ah cm}^{-2}$ at the initial cycle to 250 $\mu\text{Ah cm}^{-2}$ at the final 250th cycle.

1. Introduction

Current collector plays a crucial role in electrochemical processes in battery systems due to its indispensability as an electrical connection between electrode and external circuits. The currently used current collectors are usually two-dimensional (2D) foils incapable of accommodating a high amount of active material. In contrast with the conventional 2D current collectors, three-dimensional (3D) current collectors may offer a higher surface area keeping the equivalent volume. It is established that the use of the 3D architecture of electrodes allows to effectively increase the capacity and specific power of lithium-ion batteries (LIBs) [1]. Furthermore, in such systems, for example, metal foams, interconnected networks of open channels provide both

electronic and ionic paths, which allow efficient transfer of charge and mass transfer during repeated charging-discharging cycling. Since the specific active surface area of 3D electrodes remains high even upon increase of active material content per volume unit [2], batteries with such electrodes are able to store more energy with minimal dimensions, without losing power [3]. This gives these batteries an advantage for use in portable electronics [4].

Currently, energy and power densities of commercial batteries are limited by the low specific capacity of commonly used anodes, such as graphite. Its theoretical specific capacity, 372 mAh g⁻¹, is reached by an electrochemical formation of a compound LiC₆. Graphene (GF) is an amazing material often used as a conductive additive in composite electrodes due to its ability to provide high electric

*Corresponding author. E-mail: zbakenov@nu.edu.kz

conductivity [5]. In addition, GF is electrochemically active toward lithium with a theoretical capacity of 744 mAh g^{-1} , resulting from double-side lithiation forming LiC_3 , and a low discharge potential [6, 7]. However, it was reported that anodes based on incommensurate GF or disordered carbons are able to achieve a capacity three-four times higher than for conventional graphite owing to the fact that lithium ions can occupy the adjacent sites of GF sheets with the formation of LiC_2 intercalates [8, 9, 10]. Another anode material, nickel oxide (NiO), is one of the most investigated conversion electrode materials for LIBs due to its high theoretical capacity of 718 mAh g^{-1} , natural abundance, and low cost [11]. Nickel is a material that is known for its catalytic activity and ability to absorb carbon atoms and release them onto its surface, forming well-ordered GF layers [12].

Although the numerous studies were devoted to the use of GF-based anode in LIBs, in most cases the subject of study was the reduced GF oxide prepared by the exfoliation method [13–15]. Therefore, it was interesting to see the performance of a binder-free high purity GF, which is attached to a metal substrate. Only a few papers were published where a similar approach was considered [16, 17], and a separate electrochemical study of a grown GF, in particular, cycling performance, was incomplete.

Herein, we report on the electrochemical performance of GF grown by chemical vapor deposition (CVD) on the surface of 3D nickel foam as an anode for LIBs. In fact, this work serves as a continuation and clarification of the works reported earlier where silicon was deposited on a GF coated Ni foam [18]. Ni foam was chosen as a 3D catalyst due to its ability to produce large surface and defect-free GF layers [10] with stable scaffold in comparison with Cu foam [19]. Stability of a GF thin film is important from the point of view of its responsibility for improvement of electronic transfer in the anode as a highly conductive current collector [20]. The results of the electrochemical tests of GF on Ni foam in lithium cell showed that both, GF and the NiO native layer on Ni foam contribute to the overall capacity of the 3D structured electrode.

2. Experimental section

2.1. Material synthesis

GF was deposited onto the 3D scaffold of nickel (Ni) foam, serving as an interconnected catalytic

template owing to the surface-catalyzed mechanism of graphene growth on Ni, via a CVD method [18, 19]. Ni foam had a thickness of 1.6 mm and a porosity of $\geq 95\%$ with the average hole diameter of 0.22 mm (Goodfellow Inc.). Ni foam was cleaned by immersing in ethanol prior to CVD. Before injection of the methane-containing gas mixture (10% CH_4 + 90% Ar), an annealing was carried out in argon with hydrogen mixture (95% Ar + 5% H_2) at 200°C for 30 min to remove moisture from the catalyst surface. After this, the precursor gas mixture was injected into the reactor, and the decomposition of CH_4 took place under an ambient pressure for 5 min to provide sufficient time for carbon absorption by Ni. During cooling, graphene formed on the surface of Ni [21]. The mass increment due to the formation of GF was controlled by weighting on ultra-microbalance before and after deposition and constituted around $0.41 \pm 0.02 \text{ mg cm}^{-2}$ (Sartorius, MSE2.7S-000-DM).

2.2. Characterization

Chemical and phase composition of the samples were recorded by Raman spectroscopy on the LabRAM HR Evolution spectrometer (HORIBA Scientific) using an Ar ion 532 nm excitation laser. Morphology and microstructure of the samples were observed by a scanning electron microscope (SEM, Zeiss Crossbeam 540) at 4 kV.

2.3. Cell assembling and electrochemical test

Electrochemical tests were performed in CR2032 type coin cells assembled in an Ar-filled glove box (MBraun LABmaster Pro, $\text{H}_2\text{O} < 0.1 \text{ ppm}$ and $\text{O}_2 < 0.1 \text{ ppm}$). The electrolyte was 1 M LiPF_6 in 1:1:1 v/v/v ethylene, diethyl, and ethyl methyl carbonates (EC : DEC : EMC), a polypropylene membrane (Celgard® 2400) as a separator, a lithium metal foil as both counter and reference electrodes. The cells with Ni and GF-Ni anodes were tested for comparison of electrochemical behavior by cyclic voltammetry (CV). CV was recorded at a scan rate of 0.1 mV s^{-1} in a potential range of 0–3 V. Galvanostatic charge-discharge measurements were conducted within cut-off potentials 0.1–4 V at the current density of $30 \mu\text{A cm}^{-2}$ at ambient temperature on a battery testing system from Neware Technology Ltd. All potentials are presented vs. Li/Li^+ . The estimation of NiO native layer contribution to the overall capacity was complicated due to the absence of data

on its exact mass. Therefore, the capacity was presented as areal capacity. However, the approximate specific capacity calculated per mass of GF is provided below in the brackets as well.

3. Results and discussion

The microstructures and morphologies of the samples before and after CVD were observed by SEM. Figure 1a,b demonstrate high and low magnification images of the surface of Ni foam and its wires after cleaning by acetone prior CVD. One can see in Fig. 1b the distinguishable surface grain boundaries. As shown in Fig. 1c,d, illustrating the sample after CVD, the appearance of a dark film, consisting of numerous GF sheets, can be detected on the Ni foam surface. GF layers replicate the shape of boundaries over the Ni wires surface. The GF sheets are uniformly distributed over the Ni foam surface. In some regions, GF sheets detached from the Ni foam surface as it can be observed in the upper part of Fig. 1d. However, detached GF sheets are low in number and could be caused during handling of the sample upon preparation for SEM.

The Raman spectrum of GF film is presented in Fig. 2. Two sharp peaks centered at around 1579 cm^{-1} and 2696 cm^{-1} can be assigned to the so-called G and 2D carbon bands, respectively. The first-order D peak, usually having the shift position of around 1350 cm^{-1} , was not observed because of high purity and well-ordered structure of the synthesized graphene. In accordance with the literature data, three and more-layered GF have the 2D/G ratio less than 3 [22, 23]. This ratio for GF spectrum shown in Fig. 2 is equal 3. However, this spectrum was recorded for one point on the sample. In fact, this ratio varied from 0.75 to 3 when the Raman spectrum at different points of the sample was measured. The full width half maximum (FWHM) of the G band also can be used to identify the number of the GF layers. For example, for a single GF layer, it is $20\text{--}30\text{ cm}^{-1}$, while the FWHM of the G band for a four and five layered GF exceeds 70 cm^{-1} [24]. In the spectrum of our sample, the FWHM is within a range of $20\text{--}80\text{ cm}^{-1}$. Thus, the analysis of the G and 2D bands' features in the Raman spectra of the GF film, synthesized on the Ni foam, confirms that the samples are the few-layered GF with high quality and purity.

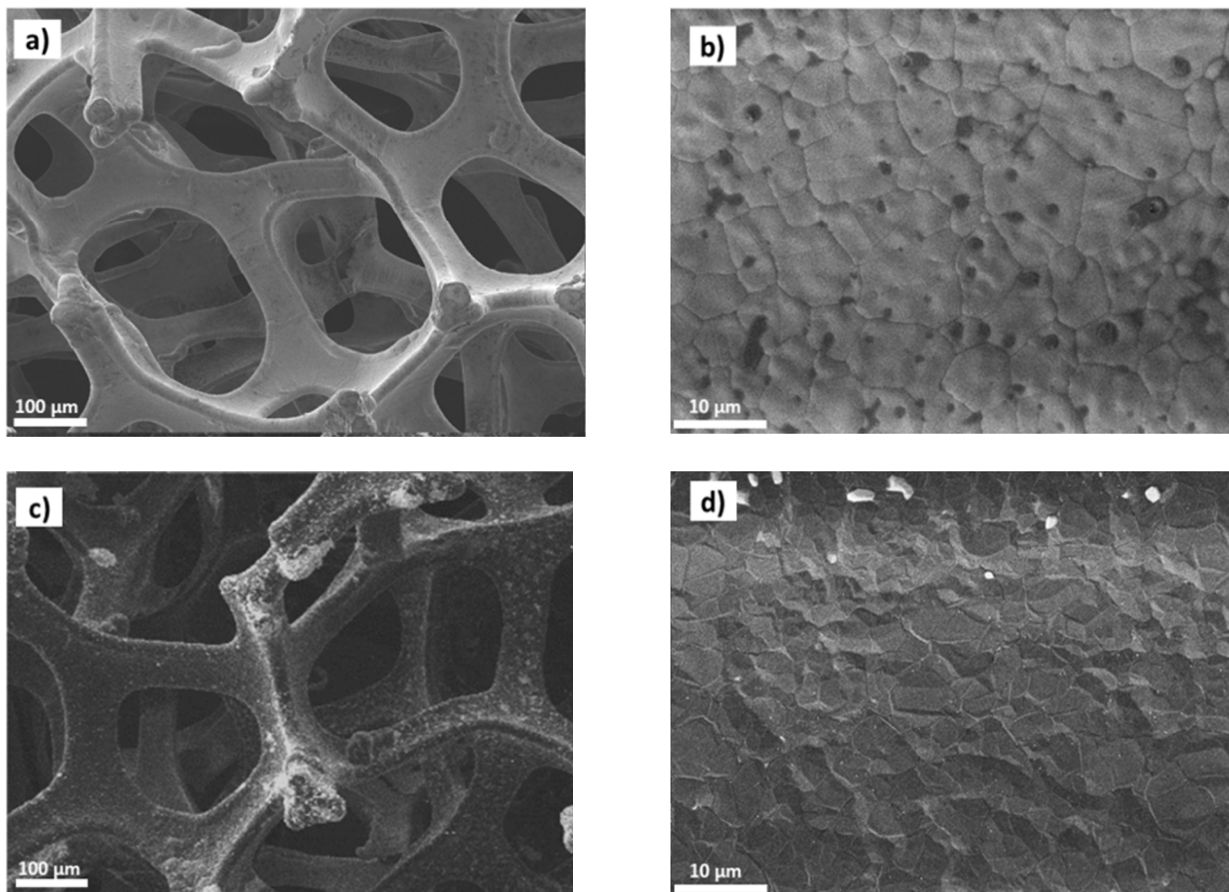


Fig. 1. SEM images of (a, b) pristine Ni foam, and (c, d) GF deposited on Ni foam.

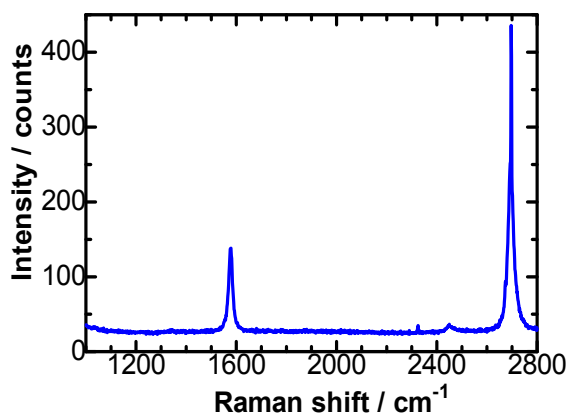


Fig. 2. Raman spectrum of GF.

In order to evaluate the feasibility of the prepared anodes for use in LIBs, the performance of the few-layered GF-Ni samples was investigated by electrochemical testing in coin-type half lithium cells. Figure 3 shows CV curves of the samples measured at a scan rate of 0.01 V s^{-1} within a potential range of 0.01–3 V. In order to distinguish the peaks coming from the current collector itself, the CV curves of Ni foam were recorded as well. In Fig. 3a, the peaks appeared at around 1.37 V and 1.23 V were related to the initial insertion of lithium ions into the NiO native layer of Ni foam followed by a displacement process with formation of Li_2O and reduction of NiO to Ni [25, 26]. This reaction is accompanied by a decomposition at oxidation of Li_2O and a return to NiO and lithium ion at 1.3 V and 2.5 V [27]. Figure 3b demonstrates the peaks of GF lithiation/delithiation: the initial solid electrolyte interface (SEI) layer formation reflected by a peak at 0.7 V, disappearing in the consequent cycles, the main reduction peaks at around

0.1 V and 0.01 V, and the oxidation peak at around 0.25 V [28–30]. Thus, in the prepared anode system, two materials – GF and NiO were recorded to be electrochemical active against lithium. However, comparing both CV graphs, recorded under the same conditions for the initial two cycles, we can see that intensities of NiO lithiation/delithiation peaks are much lower than those for GF.

Figure 4 shows the galvanostatic cycling results of the as-prepared GF-Ni sample recorded at a current rate of $30 \mu\text{A cm}^{-2}$ within 0.1–4 V. Figure 4a demonstrates the potential profiles with a magnified inset of the potential curves for the 1st, 10th and 100th cycles. The lithiation/delithiation plateaus correspond to the obtained CV data and were revealed to be similar for all cycles. In general, lithium ions have the insertion reactions with NiO at the potentials around 1.23 V and with GF at the potential onset around 0.2 V. The delithiation from GF can be seen to start at around 0.2 V and delithiation from NiO occurs at the potentials of 1.3 V and 2.5 V. From the potential profiles, it can be seen that the lithiation and delithiation peaks of NiO can be observed in all cycles. Moreover, if we compare the 100th and 250th charge curves, it can be clearly seen that the duration of NiO–Li reaction increases significantly. At the same time, the GF film has a more significant contribution to the capacity during the initial 100 cycles than NiO. Besides, the GF intercalation ability increases upon cycling as well that can be evidenced by extension of the GF delithiation plateau. Thus the overall capacity of the first charge constituted of around $65 \mu\text{Ah cm}^{-2}$ (see the inset of Fig. 4a), where GF contributed mainly. In fact, in the initial cycles, the capacity from GF was around $65 \mu\text{Ah cm}^{-2}$ (155 mAh g^{-1}), corresponding to that of graphite,

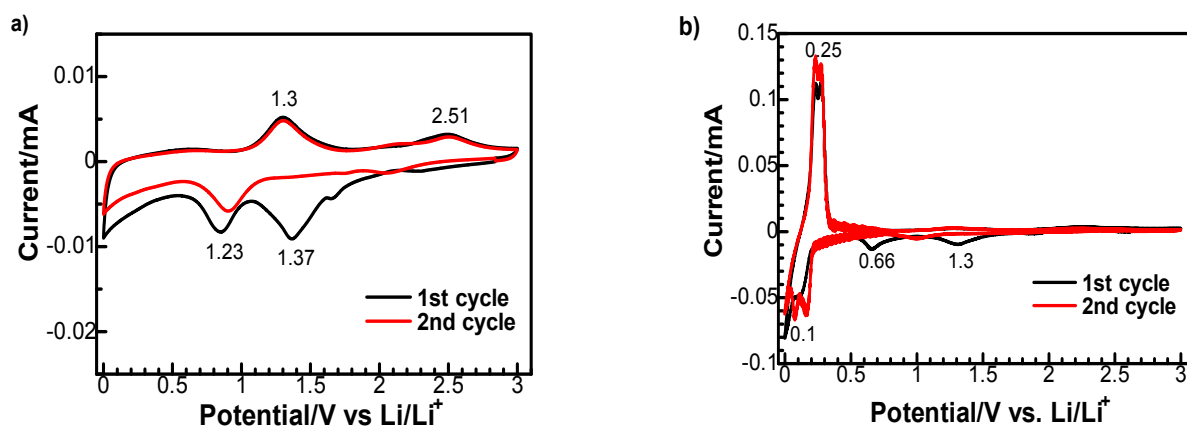


Fig. 3. CV plots of (a) Ni, and (b) GF-Ni.

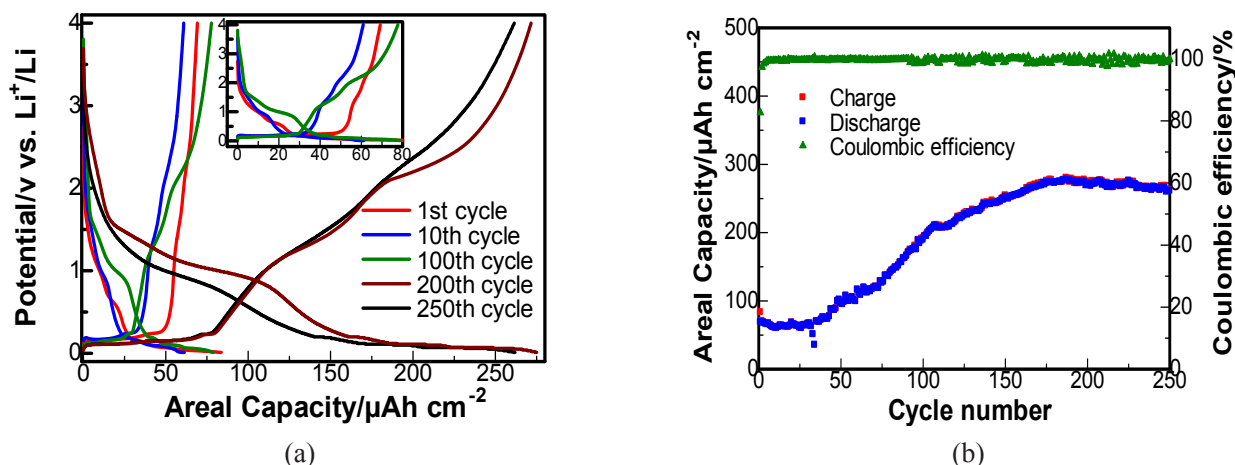


Fig. 4. (a) Potential profiles of synthesized GF with magnified inset; (b) cycling performance of GF coated Ni foam.

and increases up to $80 \mu\text{Ah cm}^{-2}$ (195 mAh g^{-1}) upon a prolonged cycling. In the last recorded 250th cycle, the cell retained the overall capacity of $250 \mu\text{Ah cm}^{-2}$ (610 mAh g^{-1}), where the duration of the delithiation reactions beyond the GF delithiation reaction range was significantly longer. Figure 4b demonstrates the cycling performance of the GF coated Ni foam anode system, where the increase of the areal capacity with a sharp climb after the 75th cycle can be observed. In general, the designed GF coated NiO/Ni electrode showed a high areal capacity of $250 \mu\text{Ah cm}^{-2}$ and a Coulombic efficiency of around 98.5% at the 250th cycle due to the electrochemical activity of the high-quality GF film and NiO layer as well as advantages of the 3D structure of anode system described above. The error in the samples' mass, determined as 0.02 mg cm^{-2} , affects the presented value of the GF-Ni foam specific capacity, especially in the last cycles, and the real value of the specific capacity in the last cycle can be in the range from 581 to 641 mAh g^{-1} .

We suppose that the gradual activation of GF upon cycling occurs due to the progressive loss of contact between GF and Ni foam, which results in additional GF sites available for lithium ions. At the same time, there is a possibility that the obtained GF degrades upon the repetitive charge/discharge cycles, and becoming less ordered, which leads to a capacity increase in carbon materials as reported in the works [6–8], leads to a capacity increase. Meanwhile, disclosed NiO layer on Ni foam starts to participate in the electrochemical reaction. It is known that the main challenge of the NiO anode is a fast capacity fading [11]. We assume that the 3D structure of anode may decrease/mitigate the NiO volume expansion. However, even a small

expansion of NiO during lithiation [31] can affect the space between GF and NiO/Ni, that gradually spreads upon cycling opening new sites of NiO layer and GF sheets for electrochemical interaction.

As it was mentioned above, the presented work was initially performed to give the additional insights for the previously reported results for the Si thin film on GF coated Ni foam [18]. The capacity of a 400 nm thick Si thin film anode on pure Ni foam reduced upon cycling from the initial capacity of $93 \mu\text{Ah cm}^{-2}$ to $33 \mu\text{Ah cm}^{-2}$ in the 250th cycle. Meanwhile, the areal capacity of Si-G-Ni anode constituted $70 \mu\text{Ah cm}^{-2}$ in the 250th cycle. Taking into account that $250 \mu\text{Ah cm}^{-2}$ was delivered by GF-Ni in the same cycle, we can qualitatively estimate that graphene has more contribution at this cycle in the Si-GF-Ni anode system. However, according to the potential profiles of the Si-GF-Ni and the GF-Ni anodes, we can see the difference between them, which is related to the contribution of the NiO/Ni component. Thus, in the latter anode (Fig. 4a), the NiO lithiation/delithiation plateaus were more expressed. Therefore, the high capacity value in the GF-Ni anode in contrast with the Si-GF-Ni can be caused by the additional capacity contribution from NiO on the surface of Ni foam.

Based on the obtained results, we can suppose that the stability of the system Si-GF-Ni foam resulted from the increasing capacity behavior of the GF and NiO layers. This finding can be very useful to develop a high capacity and stable anode using other electrode active materials. The designed and investigated GF coated Ni foam can be used not only for Si thin film anodes but in other anode systems with the high capacity materials like tin or germanium, and can enable its application in LIBs

due to abundance of available spaces in 3D structured electrodes that will help to accommodate the volume changes of the materials during lithiation/delithiation processes [32].

4. Conclusions

In this work, we report on a synthesis of a high-quality few-layered GF on Ni foam by CVD. In order to evaluate electrochemical performance of the prepared material as a negative electrode for LIBs, various electrochemical tests were carried out. It was detected that both synthesized few-layered GF and NiO native layer on Ni foam contribute to the overall capacity of the anode. The designed 3D anode demonstrated an increasing capacity behavior over a prolonged cycling starting from the initial areal charge capacity of around $65 \mu\text{Ah cm}^{-2}$ and retaining the charge capacity of around $250 \mu\text{Ah cm}^{-2}$ at the 250th cycle with a Coulombic efficiency of 98.5%. We suppose that the increasing capacity behavior of the GF coated NiO/Ni anode upon cycling occurs due to the appearance of new sites of NiO layer and GF sheets upon lithiation/delithiation reactions.

Acknowledgments

This research was funded under the targeted program 0115PK03029 “NU-Berkeley strategic initiative in warm-dense matter, advanced materials and energy sources for 2014-2018”, the research grant AP05133706 “Innovative high-capacity anodes based on lithium titanate for a next generation of batteries” and AP05133519 “Development of 3-dimensional thin film silicon based anode materials for next generation lithium-ion microbatteries” from the Ministry of Education and Science of the Republic of Kazakhstan. A. Mukanova thanks the Ph.D. Program Grant from the Ministry of Education and Science of the Republic of Kazakhstan.

References

- [1]. J.W. Long, B. Dunn, D.R. Rolison, H.S. White, *Chem. Rev.* 104 (2004) 4463–4492. DOI: 10.1021/cr020740l
- [2]. T.S. Arthur, D.J. Bates, N. Cirigliano, D.C. Johnson, P. Malati, J.M. Mosby, E. Perre, M.T. Rawls, A.L. Prieto, B. Dunn, *MRS Bull.* 36 (2011) 523–531. DOI: 10.1557/mrs.2011.156
- [3]. B. Tolegen, A. Adi, A. Aishova, Z. Bakenov, A. Nurpeissova, *Today Proc.* 4 (2017) 4491–4495. DOI: 10.1016/j.matpr.2017.04.021
- [4]. A. Mukanova, A. Jetybayeva, S.-T. Myung, S.-S. Kim, Z. Bakenov, *Today Energy.* 9 (2018) 49–66. DOI: 10.1016/j.mtener.2018.05.004
- [5]. F. Su, C. You, Y. He, W. Lv, W. Cui, F. Jin, B. Li, *J. Mater. Chem.* 20 (2010) 9644–9650. DOI: 10.1039/c0jm01633k
- [6]. H. Sun, A.E.D.R. Castillo, S. Monaco, A. Capasso, A. Ansaldo, M. Prato, D.A. Dinh, V. Pellegrini, B. Scrosati, L. Manna, F. Bonaccorso, *J. Mater. Chem. A.* 4 (2016) 6886–6895. DOI: 10.1039/C5TA08553E
- [7]. F.J. Sonia, M.K. Jangid, B. Ananthoju, M. Aslam, P. Johari, A. Mukhopadhyay, *J. Mater. Chem. A Mater. Energy Sustain.* 5 (2017) 8662–8679. DOI: 10.1039/C7TA01978E
- [8]. T.M. Paronyan, A.K. Thapa, A. Sherehiy, J.B. Jasinski, J.S.D. Jangam, *Sci. Rep.* 7 (2017) 39944. DOI: 10.1038/srep39944
- [9]. C. Bindra, *J. Electrochem. Soc.* 145 (1998) 2377. DOI: 10.1149/1.1838646
- [10]. K. Sato, M. Noguchi, A. Demachi, N. Oki, M. Endo, *Science* 264 (1994) 556–558. DOI: 10.1126/science.264.5158.556
- [11]. R. Verrelli, J. Hassoun, *ChemElectroChem* 2 (2015) 988–994. DOI: 10.1002/celec.201500069
- [12]. S. Amini, J. Garay, G. Liu, A.A. Balandin, R. Abbaschian, S. Amini, J. Garay, G. Liu, A.A. Balandin, *J. Appl. Phys.* 108 (2010) 094321. DOI: 10.1063/1.3498815
- [13]. S. Goriparti, E. Miele, F. De Angelis, E. Di Fabrizio, R. Proietti Zaccaria, C. Capiglia, *J. Power Sources.* 257 (2014) 421–443. DOI: 10.1016/j.jpowsour.2013.11.103
- [14]. X.Y. Lu, X.H. Jin, J. Sun, *Sci. China Technol. Sci.* 58 (2015) 1829–1840. DOI: 10.1007/s11431-015-5927-8
- [15]. J. Zhu, R. Duan, S. Zhang, N. Jiang, Y. Zhang, J. Zhu, *Springerplus.* 3 (2014) 585–593. DOI: 10.1186/2193-1801-3-585
- [16]. G. Radhakrishnan, P.M. Adams, B. Foran, M.V. Quinzio, M.J. Brodie, *APL Mater.* 1 (2013) 062103. DOI: 10.1063/1.4834735
- [17]. F. Li, H. Yue, Z. Yang, X. Li, Y. Qin, D. He, *Mater. Lett.* 128 (2014) 132–135. DOI: 10.1016/j.matlet.2014.04.114
- [18]. A. Mukanova, A. Nurpeissova, A. Urazbayev, S. Kim, M. Myronov, Z. Bakenov, *Electrochim. Acta.* 258 (2017) 800–806. DOI: 10.1016/j.electacta.2017.11.129
- [19]. Z. Chen, W. Ren, L. Gao, B. Liu, S. Pei, H. Cheng, *Nat. Mater.* 10 (2011) 424–428. DOI: 10.1038/nmat3001
- [20]. N. Li, Z. Chen, W. Ren, F. Li, H. Cheng, *Proc. Natl. Acad. Sci. USA* 109 (2012) 17360–17365. DOI: 10.1073/pnas.1210072109
- [21]. L. Baraton, Z.B. He, C.S. Lee, C.S. Cojocar, Marc Châtelet, J.-L. Maurice, Y.H. Lee, D.

- Pribat, *EPL – Europhysics Lett.* 96 (2011) 46003. DOI: 10.1209/0295-5075/96/46003
- [22]. S. Thiele, A. Reina, P. Healey, J. Kedzierski, P. Wyatt, P.-L. Hsu, C. Keast, J. Schaefer, J. Kong, *Nanotechnology* 21 (2010) 15601. DOI: 10.1088/0957-4484/21/1/015601
- [23]. A. Mukanova, R. Tussupbayev, A. Sabitov, I. Bondarenko, R. Nemkaeva, B. Aldamzharov, Z. Bakenov, *Mater. Today Proc.* 4 (2017) 4548–4554. DOI: 10.1016/j.matpr.2017.04.028
- [24]. Y. Hao, Y. Wang, L. Wang, Z. Ni, Z. Wang, R. Wang, C.K. Koo, Z. Shen, J.T.L. Thong, *Small*. 6 (2010) 195–200. DOI: 10.1002/sml.200901173
- [25]. G. Evmenenko, T.T. Fister, D.B. Buchholz, Q. Li, K.S. Chen, J. Wu, V.P. Dravid, M.C. Hersam, P. Fenter, M.J. Bedzyk, *Mater. Interfaces*. 8 (2016) 19979–19986. DOI: 10.1021/acsami.6b05040
- [26]. P. Poizot, S. Laruelle, S. Grugeon, L. Dupont, J. Tarascon, *Nature* 407 (2000) 496–499. DOI: 10.1038/35035045
- [27]. L. Cao, D. Wang, R. Wang, *Mater. Lett.* 132 (2014) 357–360. DOI: 10.1016/j.matlet.2014.06.114
- [28]. F.J. Sonia, M.K. Jangid, B. Ananthoju, M. Aslam, P. Johari, A. Mukhopadhyay, *J. Mater. Chem. A Mater. Energy Sustain.* 5 (2017) 8662–8679. DOI: 10.1039/C7TA01978E
- [29]. A.P. Cohn, L. Oakes, R. Carter, S. Chatterjee, A.S. Westover, K. Share, C.L. Pint, *Nanoscale* 6 (2014) 4669. DOI: 10.1039/C4NR00390J
- [30]. F. Ding, W. Xu, D. Choi, W. Wang, X. Li, M.H. Engelhard, X. Chen, Z. Yang, J.-G. Zhang, *J. Mater. Chem.* 22 (2012) 12745–12751. DOI: 10.1039/c2jm31015e
- [31]. A. Rahman, C. Wen, *Ionics*. 22 (2016) 173–184. DOI: 10.1007/s11581-015-1542-8
- [32]. C. Zhao, S. Li, X. Luo, B. Li, H. Wu, *J. Mater. Chem. A*. 3 (2015) 10114–10118. DOI: 10.1039/C5TA00786K